NUREG/CR-0301
BNL-NUREG-50880

PRELIMINARY INVESTIGATION OF TURBULENT REACTIVE MIXING IN PCRV/CV GAS MIXTURES

J.L. Boccio

Date Published - August 1978

HTGR SAFETY DIVISION
DEPARTMENT OF NUCLEAR ENERGY, BROOKHAVEN NATIONAL LABORATORY
UPTON, NEW YORK 11973

Prepared for the U.S. Nuclear Regulatory Commission
Office of Nuclear Regulatory Research
Contract No. EY-76-C-02-0016

NUREG/CR-0301
BNL-NUREG-50880
R-8

PRELIMINARY INVESTIGATION OF TURBULENT REACTIVE MIXING IN PCRV/CV GAS MIXTURES

J.L. Boccio

Manuscript Completed - May 1978
Date Published - August 1978

HTGR SAFETY DIVISION
DEPARTMENT OF NUCLEAR ENERGY
BROOKHAVEN NATIONAL LABORATORY
ASSOCIATED UNIVERSITIES, INC.
UPTON, NEW YORK 11973

PREPARED FOR THE UNITED STATES NUCLEAR REGULATORY COMMISSION
DIVISION OF REACTOR SAFETY RESEARCH, OFFICE OF NUCLEAR REGULATORY RESEARCH
UNDER CONTRACT NO. EY-76-C-02-0016
NRC FIN NO. A-3016

NOTICE

Available from
U.S. Nuclear Regulatory Commission
Washington, D.C. 20555

Available from
National Technical Information Service
Springfield, Virginia 22161

ABSTRACT

Relaxation of the prima facie assumption of complete mixing of primary containment and secondary containment gases during postulated depressurization accidents within gas cooled reactors has led to a study program designed to identify and selectively quantify the relevant gas dynamic processes which are manifest during the depressurization event. Uncertainty in the degree of gas mixedness naturally leads to uncertainty in containment vessel design pressure and heat loads and possible combustion hazards therein. This report details an analytical approach in the modeling of the exhaust-jet structure during a penetration failure. A chemical kinetics model is also described for the possibility of examining diffusive flame structure assuming the exhaust jet is composed of combustibles as well.

The salient features of the mixing model and associated reaction kinetics are embodied in the classical problem of a turbulent, chemically reacting jet exhausting into a stationary ambient atmosphere capable of supporting combustion. A so-called "two equation" turbulence model is linked to a chemical kinetics code describing the production of CO_2 and H_2O with He and N_2 considered as inert diluents. The usefulness of the model is exemplified by experimental/numerical comparisons presented in the open literature and within this report. The need for such a calculational tool in HTGR safety research is stressed as well.

TABLE OF CONTENTS

LIST OF FIGURES

LIST OF TABLES

SECTION I

INTRODUCTION

Analysis of high temperature gas-cooled reactor (HTGR) plant response under normal, upset and accident conditions requires an overall simulation of major plant components in which interaction between components and systems are realistically taken into account. This is, for example, the basic premise behind the TAP code[1]. However, in order to hold the program to a manageable size necessitates the use of simplified submodels for some of the more complex portions of the system. More detailed models of individual subsystems have been derived to continuously check the overall reliability of this approach. For example, the OXIDE-3 code[2] is a third generation computer code developed for the purpose of analyzing the transient reactor core response following accidental inleakage of steam and/or air to the primary coolant system. The CONTEMP-G[3] computer program was developed to simulate containment atmospheric response to postulated penetration failures within the prestressed concrete reactor vessel (PCRV) under the assumption of complete and homogeneous mixing of PCRV coolant and containment vessel (CV) atmosphere. A refinement thereof is modelled with the HTGRF4[4] and HAZARD[5] codes, wherein the possibility for, and consequences of, primary coolant layering due to incomplete, albeit pre-specified, mixing is examined. Specifically, (a) the question of the flammability hazards within the PCRV due to CV gas inleakage after penetration failure[4], or (b) the question of the flammability within the CV during a penetration failure[5] are addressed under the assumptions of homogeneous or partial PCRV/CV gas "mixedness" and instantaneously fast chemical reaction kinetics.

Notwithstanding, the extreme remoteness of an occurrence resulting from the question posed by statement (b) above, which presupposes that combustibles, viz., H_2/CO are generated within the PCRV due to water/steam leakage prior to a penetration failure, the relative ease in extending a binary gas (He/Air) containment response code into a multicomponent gas (He/Air/CO/H_2) response code warranted its subsequent investigation.

Regardless, the presumption in knowing the degree of PCRV/CV gas "mixedness" (either fully mixed as in CONTEMP-G or partially mixed as in HAZARD), and the assumption of chemical equilibrium amongst gas specie components requires further investigation with codes which realistically model the subsequent turbulent mixing of PCRV gas with CV gas and possible concomitant chemical reaction kinetics. In particular, these two factors,

- turbulent, diffusive mixing
- finite-rate chemical kinetics

are extremely relevant in the investigation of post-penetration failures, especially if gas layering is indeed probable. In this regard, it is quite likely that fluid-mechanic flow times in turbulent, buoyant plumes are comparable to chemical reaction times, necessitating investigations in diffusion-controlled as well as chemically-controlled mixing processes. Furthermore, it is felt that as a precursor in the investigation of detonability within large vessels, experience accrued in turbulent, reactive mixing is of paramount importance.

Accordingly, this report deals specifically in numerically modeling free, turbulent, reactive shear layers. As a subprogram, it has direct application in extending existing codes specifically designed in penetration failure studies. Also, the main thrust in the numerical approach has bearing in the study of buoyant plumes and buoyant wall-jets, fission product release and accompanying

deposition. Accordingly, Section II deals wholly with the basic governing differential equations generally used in describing turbulent, reactive shear flows. Along with the basic conservation equations of mass, momentum and energy, a well-tried turbulence model and turbulence modeling phenomenology are also discussed. As a preface to the numerical technique, a mapping transformation of the independent variables is described in Section III indicating, from a numerical standpoint, its relevance in modeling flows with free boundaries. A hybrid implicit/explicit numerical technique is described in Section V. The need for such a mixed finite-difference approach when considering reactive flows is also discussed in this section. A description of the chemical-kinetic rate mechanism for a $H_2/CO/O_2$ system with He and N_2 considered as inert dilutants is presented in Section VI. One major aspect of the overall approach, namely, that the numerical code is not restricted to only this kinetics scheme, is also emphasized. Section VII exhibits some numerical/experimental comparisons for nonreactive, diffusive flows, indicating the efficacy in the turbulence model and the numerical approaches used. Section VIII is devoted to a qualitative interpretation of select numerical experiments in reactive flows; problem areas are defined and means of code augmentation discussed throughout. Finally, Section IX reemphasizes the need for such a mathematical tool in HTGR reactor safety and elaborates further its possible use in other areas pertaining thereto.

SECTION II

GOVERNING EQUATIONS FOR TURBULENT REACTIVE SHEAR FLOWS

Conceptually, methods exist for solving the equations for unsteady, three-dimensional flows, which are in principle capable of predicting the details of any turbulent flow, by starting with the highly reliable Navier-Stokes equations. However, the practical possibility of utilizing these numerical techniques is, presently, very small because of the great disparity of scale between the size of most practical flow domains and the sizes of the turbulent fluid eddy structure. To circumvent this scale disparity problem, which manifests itself by the employment of an impractical fine grid network for numerical computation of even the most simplest of turbulence flow phenomena, investigators, in the consequences of turbulence in flows of practical engineering interest, have resorted to the use of various "turbulence models".

In general, these are sets of equations which attempt to describe the convective transport, the diffusion, the generation and the decay of certain statistical properties of a turbulent fluid -- the so-called "correlations". Particularly, the subject of turbulence modeling of free shear layers has, in recent years, received a considerable amount of attention.[6,7,8] A major consequence of these studies is the general agreement that turbulence models which include within the describing set of partial differential equations a means for also determining the transport of turbulent kinetic energy yield results which are superior to those relying on local eddy-viscosity assumptions (i.e., "algebraic" models of turbulence). Although a hierarchy of such models has been developed, ranked according to the number of additional differential equations solved simultaneously to describe the mean and fluctuating structure within shear layers, most emphasis has been placed upon the "two-equation

turbulence models" which describe the approximate transport of turbulent kinetic energy, k, and its dissipation rate, ε. These are solved in conjunction with the usual equations describing the transport of mean momentum, energy and mass. The link between the "apparent" eddy transport coefficients, e.g., eddy viscosity, appearing in the mean conservation equations as a result of the usual Eulerian time-averaging techniques applied to the Navier Stokes equations, is made using algebraic, constitutive equations directly relating these turbulence transport coefficients to the turbulent kinetic energy and dissipation rate.

In this regard, the problem under consideration, that is, the free turbulent mixing of two chemically reacting, co-axial streams (Figure 1) involving N chemical species made up from L elements and undergoing R chemical reactions, is addressed using a two-equation turbulence model that has been extensively investigated by Spalding and his co-workers at the Imperial College[8,9].

II.1 The Mean Flow Conservation Equations

For compressible turbulent flows, the equations describing the transport of mean momentum, energy and mass are, in principle, derived in a similar fashion as those for incompressible turbulent flows. The mean velocity field follows from the Navier Stokes equations by the usual decomposition of the velocity vector, u_i, into mean and fluctuating components, $u_i = \bar{u}_i + u_i'$ $(i = 1,2,3)$, and application of standard time-averaging techniques. The resulting equations for the mean velocity field, $\bar{u}_i$, have, in general, the same form as the original Navier Stokes equations except for the addition of the apparent turbulent stress terms (Reynolds stresses) which, written in cartesian tenser notation, have the form $\overline{\rho u_i' u_j'}$ ($\rho \equiv$ density). To close this system, additional equations must be sought for the second order correlation terms $R_{ij} \equiv (\overline{u_i' u_j'})$, usually provided by the

Newtonian constitutive relation $R_{ij} = (2/3)(k^2)(S_{ij}) - 2\mu_T S_{ij}$, where S_{ij} is the usual strain rate tensor given by $S_{ij} = 1/2(\partial\overline{u}_i/\partial x_j + \partial\overline{u}_j/\partial x_i)$, k^2 is the turbulent kinetic energy defined by $k^2 = 1/2\ R_{ii}$, and μ_T is the turbulent eddy viscosity. An equation describing the dynamics of the turbulence kinetic energy can also be derived from the Navier-Stokes equations by the following procedure: (1) multiplying the x_i component of the Navier-Stokes equation by u_j', (2) multiplying the x_j component of the Naver-Stokes equation by u_i, (3) adding the two resulting equations, (4) time-averaging, and finally (5) resorting to tensor contraction. The resulting equation is quite complex, including triple order ($\overline{u_i' u_j' u_\ell'}$) correlations, and means for making this equation more tractable are discussed by Bradshaw and others[10].

For compressible flows, the situation is more complex in the sense that fluctuations in density (ρ') and temperature (T') must also be considered for non-reacting flows and, most recently[6], concentration fluctuations in multi-component, reacting flows as well. The scope of this study does not lend itself to the elaboration of these details; one interested in further clarification can resort to the previously cited references. Accordingly, the equations to follow are simply stated without further recourse to their origin. Suffice it to say that they are considered by most investigators as the standard equations for compressible turbulent flow.

Thus, for the subject problem under discussion, we assume the mean flow to be (1) steady (or at least quasi-steady), (2) axisymmetric, and (3) well approximated by the so-called boundary-layer assumptions where gradients in the direction normal to the flow are considered much greater than those in the axial (or flow) direction. Considering the simplifying assumption of a binary Fickian diffusion law with the same diffusion coefficient for each of the

species, the resulting equations describing the transport of mean momentum, energy, mass and species are:

Momentum:*

$$\rho u \frac{\partial u}{\partial x} + \rho v \frac{\partial v}{\partial r} = r^{-1} \frac{\partial}{\partial r} \left\{ \rho r (\mu + \mu_t) \frac{\partial u}{\partial r} \right\} - \frac{dp}{dx} + g(\rho_E - \rho) \tag{1}$$

Energy:

$$\rho u \frac{\partial H}{\partial x} + \rho v \frac{\partial H}{\partial r} = r^{-1} \frac{\partial}{\partial r} \left\{ \frac{\rho r \mu_t}{Pr} \left[\frac{\partial H}{\partial r} + \left(\frac{Pr}{Pr_t} - 1 \right) \frac{\partial k}{\partial r} + (Pr-1) \frac{\partial u^2/2}{\partial r} \right. \right.$$

$$\left. \left. + \left(\frac{Pr}{Pr_t} \right) \left(Le_t - 1 \right) \sum_{i=1}^{N} h_i \frac{\partial \alpha_i}{\partial r} \right] \right\} \tag{2}$$

Mass:

$$\frac{\partial}{\partial x} (\rho u r) + \frac{\partial}{\partial r} (\rho v r) = 0 \tag{3}$$

Species:

$$\rho u \frac{\partial \alpha_i}{\partial x} + \rho v \frac{\partial \alpha_i}{\partial r} = r^{-1} \frac{\partial}{\partial r} \left\{ \frac{\rho r \mu_t}{Sc} \left(1 + \frac{\mu}{\mu_t} \right) \frac{\partial \alpha_i}{\partial r} \right\} + \dot{w}_i \tag{4}$$

$$i = 1,2,3, \ldots . N-L$$

Elements:

$$\rho u \frac{\partial \tilde{\alpha}_j}{\partial x} + \rho v \frac{\partial \tilde{\alpha}_j}{\partial r} = r^{-1} \frac{\partial}{\partial r} \left\{ \frac{\rho r \mu_t}{Sc} \left(1 + \frac{\mu}{\mu_t} \right) \frac{\partial \tilde{\alpha}_j}{\partial r} \right\} \tag{5}$$

$$j = 1,2 \ldots . L$$

---

* For clarity, the bar over each mean flow variable has been omitted.

In these equations, u and v are the mean axial (x) and radial (r) components of velocity, respectively; ρ is the mean gas density, p the pressure; H the total enthalpy; μ_t the turbulent eddy viscosity coefficient; α_i and $\tilde{\alpha}_j$ the mass fraction of species i and element j, respectively; $\dot{w}_i$ the mass rate of production of species i; Pr_t and Sc_t the turbulent enthalpy and mass exchange coefficients; Le_t the turbulent Lewis number.

The instantaneous mass rate of production* per unit volume is, through the law of mass action, given by

$$\dot{w}_i = W_i \sum_{j=1}^{R} (\nu''_{ij} - \nu'_{ij})\, k_{f,j}\, \rho^{n_j} \prod_{i=1}^{N} (\alpha_i/W_i)^{\nu'_{ij}}\, G_j \qquad (6)$$

where

$$G_j \equiv 1 - \rho_j^{m}\, K_{c,j}^{-1} \prod_{i=1}^{N} (\alpha_i/W_i)^{\nu''_{ij} \quad \nu'_{ij}}$$

$$n_j \equiv \sum_{i=1}^{N} \nu'_{ij} \qquad (7)$$

$$m_j \equiv \sum_{i=1}^{N} (\nu''_{ij} - \nu'_{ij})$$

The forward rate constant, $k_{f,j}$, and the equilibrium constant $K_{c,j}$ are based upon the molar concentrations for the j^{th} reaction expressed in the form

$$\sum_{i=1}^{N} \nu_{ij}'\, M_i \underset{k_{b,j}}{\overset{k_{f,j}}{\rightleftharpoons}} \sum_{i=1}^{N} \nu_{ij}''\, M_i \qquad j = 1,2, \ldots R \qquad (8)$$

---

* In this formulation, the phenomenological equations for the chemical kinetics do not include the effects of fluctuations in concentration and temperature.

where ν_{ij}' and ν_{ij}'' are the stoichiometric coefficients of the reaction. The fluid is assumed to be comprised of a mixture of ideal gases; thus, the equation of state is given by

$$p = \rho R_o T \sum_{i=1}^{N} \alpha_i / W_i = \rho R_o T / W \tag{9}$$

where R_o is the universal gas constant. In practice, the temperature, T, is determined by an iterative solution to the equation that defines the static enthalpy, h, of the gas mixture, i.e.,

$$h \cong H - 1/2(u^2 + v^2) = \sum_{i=1}^{N} (\alpha_i / W_i) h_i^o \ (T) \tag{10}$$

where $h_i^o(T)$ is the sum of the sensible enthalpy and chemical energy of species i at 0^oK for the standard state and is presumed given by a polynomial expression involving T, i.e.,

$$h_i^o(T) = \sum_{k=1}^{p} a_{i,k} T^{(k-1)} \tag{11}$$

Once the chemical kinetic mechanism, i.e., Equation (8), are defined and the condition that the backward rate constants $k_{b,j}$ are related to the forward rates, $k_{f,j}$, and the equilibrium constant $K_{c,j}$, the above system of equations is closed once expressions for the turbulent exchange coefficients, μ_t, Pr_t, Sc_t, Le_t and turbulent kinetic energy are derived. In practice, one usually presupposes that the turbulent exchange coefficient for heat (Pr_t) and mass (Sc_t) in gas-dynamic flows are constants and of order of unity. As such, phenomenological laws and/or equations are required to evaluate the turbulent momentum exchange coefficient, μ_t, and the turbulent kinetic energy.

In zero-equation models, μ_t is related directly to the mean velocity field u, that is, $\mu_t \sim (\Delta u)(\Delta r)$ where (Δu) is some appropriate velocity difference associated with the flow (e.g., the difference between jet center line velocity and the external flow velocity), and (Δr) is a length scale characterizing the width of the jet. Also, in zero-order modeling the turbulent kinetic energy is not considered. In one-equation turbulence models, a turbulent kinetic energy equation forms the basis for a model equation for the turbulence velocity scale with the eddy viscosity given by $\mu_t \sim k\ell_t$. The turbulent length scale, ℓ_t, is prescribed much as in the zero-equation approach. For the two-equation approach, the phenomenology is much the same as in the one-equation model, except for the fact that a differential equation is used to describe the x,r,-dependency for the length scale, ℓ_t (or equivalently the kinetic energy dissipation rate, ε[10]).

II.2 The Two-Equation Turbulence Model

One of the more widely accepted two-equation turbulence models is based upon the so-called "k-ε2" model described by Launder[8]. In this approach*, the turbulent eddy viscosity is modelled using the equation

$$\mu_t = C'_\mu \rho \ell_t k \tag{12}$$

where C'_μ is a function of the local axial velocity gradient.

---

* A refinement to the k-ε2 model is that proposed and subsequently used by Spalding (see "Concentration Fluctuations in a Round Turbulent Jet", Chem. Engr. Sci., 1971, Vol. 26). This method has found marked success in turbulent buoyant plumes, and its implementation into the present analysis is subsequently under investigation.

The turbulent length scale is shown by dimensional considerations to be related to the turbulent kinetic energy and turbulence dissipation rate, ε, via the expression

$$\varepsilon = C_\varepsilon \, k^{3/2}/\ell_t \tag{13}$$

thus requiring the turbulent viscosity to be dependent upon two properties of the fluid turbulence, namely k and ε, viz.,

$$\mu_t = C_\mu \rho k^2/\varepsilon \tag{14}$$

Transport equations for the turbulent kinetic energy and turbulent dissipation rate may be derived from the Navier-Stokes equations, employing the usual Eulerian time-average techniques used in deriving the above noted mean conservation equations. The resulting two equations require considerable modeling, however, to reduce the higher-order turbulence correlation terms that accrue due to the averaging technique to more tractable forms. Based upon heuristic, dimensional arguments, Launder shows that the two transport equations for k and ε are given by

$$\rho u \frac{\partial k}{\partial x} + \rho v \frac{\partial k}{\partial r} = r^{-1} \frac{\partial}{\partial r}\left[r \mu_T \sigma_k^{-1} \frac{\partial k}{\partial r}\right] + \mu_t \left(\frac{\partial u}{\partial r}\right)^2 - \rho\varepsilon \tag{15}$$

and

$$\rho u \frac{\partial \varepsilon}{\partial x} + \rho v \frac{\partial \varepsilon}{\partial r} = r^{-1} \frac{\partial}{\partial r}\left[r \mu_T \sigma_\varepsilon^{-1} \frac{\partial \varepsilon}{\partial r}\right] + C_{\varepsilon 1} \frac{\varepsilon}{k} \mu_t \left(\frac{\partial u}{\partial r}\right)^2 - C_{\varepsilon 2} \frac{\rho \varepsilon^2}{k} \tag{16}$$

Equations (14), (15) and (16) form the foundation of the "two-equation model" of Launder. Refinements in the five constants, viz., C_μ, $C_{\varepsilon 1}$, $C_{\varepsilon 2}$, σ_k and σ_ε, originally deduced by Launder, have been investigated by Rodi[11]. These are

incorporated herein and listed in Table I. In particular, the quantity, f, in Table I embodies an axisymmetric correction to the basic values of 0.09 and 1.94 for C_μ and $C_{\varepsilon 2}$, respectively, where

$$f = \left\{ \frac{\Delta r}{2\Delta u} \left[\left(\frac{du}{dx} \right)_{CL} - \left| \frac{du}{dx} \right|_{CL} \right] \right\}^{0.2}$$

in which Δr and Δu reflect the width and velocity change across the mixing layer. A further correction to the "constant" C_μ takes into account the fact that in weak shear flows the rate of turbulence energy production is appreciably less than the dissipation rate. In such circumstances, the value of C_μ increases, and Rodi has provided a correction for the variation in C_μ with the average value of the ratio of turbulence energy production to dissipation at any cross-section. These empirical corrections have also been included in this analysis.

Thus, the partial differential equations describing the transport of mean mass, momentum and energy, i.e., Equations (1) through (5), together with Equations (15) and (16), which approximate the transport of turbulent kinetic energy and its dissipation rate, plus the aforenoted constitutive algebraic equations form a complete set of equations for the investigation of turbulent, reactive flows. These partial differential equations are solved subject to the following initial and boundary conditions:

$$x = 0: \quad u = u(r),\ H = H(r),\ k = k(r),\ \varepsilon = \varepsilon(r), \alpha_i = \alpha_i(r),\ \tilde{\alpha}_j = \tilde{\alpha}_j(r)$$

$$r = 0 \quad \partial u/\partial r = \partial H/\partial r = \partial k/\partial r = \partial \varepsilon/\partial r = \partial \alpha_i/\partial r = \partial \tilde{\alpha}_j/\partial r = 0 \qquad (17)$$

$$r \to \infty \quad u \to u_E,\ H \to H_E,\ k = \varepsilon = 0,\ \alpha_i \to \alpha_{iE},\ \tilde{\alpha}_j \to \tilde{\alpha}_{jE}$$

Pressure p is allowed to vary in the axial direction, according to an a priori prescribed function

SECTION III

TRANSFORMATION TO MAPPED STREAM FUNCTION COORDINATES

For convenience in numerical computations, the conservation equations of mass, momentum and energy, and the second-order closure energy-dissipation model equations are recast from the physical (x,r) plane to a mapped streamline coordinate plane (x,ω) along the lines of Patankar[12]. The mapping variable, ω, is defined by

$$\omega \equiv [\psi - \psi_I(x)]/[\psi_E(x) - \psi_I(x)]$$

where E and I, respectively, represent the external and inner boundaries of the mixing zone (see Figure 1). The term $(\psi_E - \psi_I)$ is a measure of the mass flow in the mixing layer at a given x-station, i.e.,

$$\psi_E - \psi_I = \int_{r_I}^{r_E} \rho u r dr$$

By this process global continuity, i.e., Equation (3), is automatically satisfied, and by definition of the stream function, ψ, namely

$$\partial\psi/\partial r = \rho u r \quad ; \quad \partial\psi/\partial x = -\rho v r$$

the dependent variable, v, is automatically eliminated from the governing system of equations.

Thus, by first introducing the von Mises coordinate transformation

$$(x,r) \rightarrow (x,\psi)$$

into the governing differential equations, noting that

$$\frac{\partial}{\partial x} = \frac{\partial}{\partial x} + \frac{\partial}{\partial \psi}\frac{\partial \psi}{\partial x} = \frac{\partial}{\partial x} - \rho v r \frac{\partial}{\partial \psi}$$

$$\frac{\partial}{\partial r} = \frac{\partial}{\partial \psi}\frac{\partial \psi}{\partial r} = \rho u r \frac{\partial}{\partial \psi}$$

and thence introducing the mapped stream function coordinates

$$(x,\psi) \rightarrow (x,\omega)$$

into the resulting transformed equations, further noting that

$$\frac{\partial}{\partial x} = \frac{\partial}{\partial x} + (\psi_E - \psi_I)^{-1}\left[-\frac{d\psi_I}{dx} - \omega\left(\frac{d\psi_E}{dx} - \frac{d\psi_I}{dx}\right)\right]\frac{\partial}{\partial \omega}$$

$$\frac{\partial}{\partial \psi} = \frac{\partial}{\partial \omega}\frac{\partial \omega}{\partial \psi} = (\psi_E - \psi_I)^{-1}\frac{\partial}{\partial \omega}$$

yield a set of differential equations which can symbolically be represented by the vector equations:

$$\frac{\partial}{\partial x}\vec{\phi} + (a + b\omega)\frac{\partial}{\partial \omega}\vec{\phi} = \frac{\partial}{\partial \omega}\left(c_\phi \frac{\partial \vec{\phi}}{\partial \omega}\right) + \vec{d}_\phi \qquad (18a)$$

$$\vec{\phi} = (u,H,k,\varepsilon,\alpha_1,\alpha_2, \ldots \alpha_{N-L}, \tilde{\alpha}_1, \tilde{\alpha}_2, \ldots \tilde{\alpha}_2)^T \qquad (18b)$$

$$\vec{d}_\varphi = (d_u, d_H, d_k, d_\varepsilon, \ldots d_{\alpha_i}, \ldots, \ldots d_{\tilde{\alpha}_j} \ldots)^T \qquad (18c)$$

where now the dependent variables u, H, k and ε have been non-dimensionalized respectively by u_j, H_j, u_j^2, u_j^3/r_j; the pressure by p_j; the density by ρ_j; the eddy viscosity by $\rho_j u_j r_j$. Equation (18a) symbolizes a set of N+4 partial differential equations; the components of the source vector, $\vec{d}_\varphi$, for a turbulent

Lewis number, Le_t, of unity, is provided in Table II. The coefficients a, b, c_φ which result from the mapping laws are defined by:

$$a = -(d\psi_I/dx)/(\psi_E - \psi_I) = r_I m_I/(\psi_E - \psi_I) \tag{19a}$$

$$b = d/dx \left[\ln(\psi_E - \psi_I)\right] = (r_E m_E - r_I m_I)/(\psi_E - \psi_I) \tag{19b}$$

$$c_\varphi = \rho u r^2 \mu_T/\sigma_\varphi/(\psi_E - \psi_I)^2 \tag{19c}$$

where m_I and m_E represent the mass flux per unit area entrained into the mixing layer through the I-boundary and E-boundary, respectively. Methods for evaluating the expressions, $r_I m_I$, $r_E m_E$, and $\Delta\psi$ are described by Patankar and Harsha[13]. For the present study, the approach taken by Patankar is used.

SECTION IV

ENTRAINMENT OF FLUID AT A FREE BOUNDARY

The normalized stream-function coordinate has the advantage that it allows the numerical grid to automatically expand with the mixing layer, thereby always containing the relevant portion of the flow (Fig. 2). However, in order to proceed numerically, it is necessary to estimate the amount of fluid entrained into the mixing layer, both through the E-boundary (outer), and, until the lower edge of the mixing layer reaches the axis, through the I-boundary (inner) as well.

To determine the amount of mass entrained and the subsequent growth of the stream function $(\psi_E-\psi_I)$, consider Equation (18a) for $\phi_i=u$, which written out in full is:

$$\frac{\partial u}{\partial x} + \left\{ r_I m_I + \left[\frac{(r_E m_E - r_I M_I)\ \omega}{\psi_E - \psi_I} \right] \right\} \frac{\partial u}{\partial \omega} = \frac{\partial}{\partial \omega} \left\{ \frac{r^2 \rho u \mu_T}{(\psi_E-\psi_I)^2} \frac{\partial u}{\partial \omega} \right\} - \frac{1}{\rho u} \frac{dp}{dx} + g(\rho_E-\rho)$$

In the case of free mixing, the conditions at the edges of the boundary must be such that

$$\frac{\partial u}{\partial x} = - \frac{1}{\rho u} \frac{dp}{dx} + g(\rho_E-\rho)$$

since by definition the outer and inner regions are inviscid. Accordingly, in the limit $\omega \to 0$, we have

$$r_I m_I \cong \lim_{\omega \to 0} \left\{ \frac{\partial}{\partial \omega} \left[\frac{r^2 \rho u \mu_T}{(\psi_E - \psi_I)} \frac{\partial u}{\partial \omega} \right] \Big/ \frac{\partial u}{\partial \omega} \right\}$$

$$= \lim_{r \to r_I} \left\{ \frac{\partial}{\partial r} (r\mu_T) + (r\mu_T) \frac{\partial^2 u}{\partial r^2} \Big/ \frac{\partial u}{\partial r} \right\}$$

which Patankar reduces further to

$$r_I m_I = \lim_{r \to r_I} \left\{ \frac{\partial}{\partial r} (r\mu_T) \right\}$$

and, likewise, for the outer edge

$$r_E m_E = \lim_{r \to r_E} \left\{ \frac{\partial}{\partial r} (r\mu_T) \right\}$$

Thus, with the above two expressions, Equation (19b) can, in principle, be used to evaluate $(\psi_E - \psi_I)$.

SECTION V

THE NUMERICAL INTEGRATION PROCEDURE

Resorting to the mapping laws previously described, the lateral domain of the mixing region, defined by $0 \leq \omega \leq 1$ rather than by $r_I \leq r \leq r_E$, results in a system of equations having advantages both in conceptual simplicity and computational efficiency. In particular, for cases involving frozen mixing ($\dot{w}_i = 0$) or mixing with chemical equilibrium, the choice of implicit[14] or explicit[15] finite difference techniques becomes a matter of personal preference. However, in the case of chemical non-equilibrium, the potential for a system of "stiff" differential equations[16,17] due to the possibility of one or more of the chemical reactions being at or near chemical equilibrium requires one to resort to various hybrid implicit/explicit techniques[18,19].

Thomas[18] employs the MacCormack[11] predictor-corrector scheme which is second order accurate in both $\Delta x, \Delta\omega$ for all the governing equations other than the specie conservation equation. For the specie conservation equation, Thomas uses a modified predictor-corrector scheme whereby the predictor step is fully explicit, while treating the species, α_i, as chemically inert ($\dot{w}_i = 0$). The chemical production rate term, $\dot{w}_i$, is differenced in implicit fashion in the corrector, albeit the convection and turbulent diffusion terms are again differenced in an explicit fashion.

Boccio,[19] on the other hand, utilizes the implicit technique of Patankar[14] where the governing differential equations are integrated over a small control volume associated with individual grid joints in the (x,ω) plane. The resulting finite difference equations with the production terms, $\dot{w}_i$, considered for the moment zero (i.e., frozen flow) are formulated in an implicit manner and solved

by means of the well known algorithm for tri-diagonal matricies. For each grid point the chemistry is decoupled from the system by assuming

$$\alpha_K = \alpha_K^{(D)} + \alpha_K^{(C)} \qquad K = 1,2, \ldots N$$

each respectively controlled by the equations

$$\frac{\partial \alpha_K^{(D)}}{\partial x} + (a + b\omega)\frac{\partial \alpha_K^{(D)}}{\partial \omega} = \frac{\partial}{\partial \omega}\left(c\ \frac{\partial \alpha_K}{\partial \omega}\right)$$

and

$$\frac{d\alpha_K^{(C)}}{dx} = \frac{\dot{w}_K}{\rho u}$$

where the $\alpha_K^{(D)}$ comprise a subset of the dependent variable column vector $\vec{\phi}$ for the frozen flow ($\dot{w}_i = 0$; $d_{\alpha_i} = 0$) subsystem of equations. The above one-dimensional finite rate chemistry equation along a stream line within the integration step can be solved using the linearized technique of Moretti[20] or Rubel[21] or the Pade method of Magnus and Schecter.[22] The present method, however, incorporates the method of Moretti and Rubel in uncoupling and solving for finite rate kinetics.

V.1 Finite Difference Equations: (Interior Points, $\dot{w}_i = 0$)

With reference to the computational grid network and notation of Figure 3, the micro integral over the element $(i, j+\frac{1}{2})$, $(i-1, j+\frac{1}{2})$, $(i-1, j-\frac{1}{2})$, $(i, j-\frac{1}{2})$ is performed assuming:

- φ varies linearly between adjacent cross-stream steps,

  that is, $\omega = \omega_{i,\ j+\frac{1}{2}}$;

$$\varphi = \tfrac{1}{2}\left(\varphi_{i,j} + \varphi_{i,j+1}\right).$$

- φ varies in a stepwise manner between adjacent stream-wise steps, i.e., $x_{i-1} < x \leq x_i$

$$\varphi = \varphi_{i,j}$$

The micro-integral of Equation (18a), using the above assumptions, has the following components

$$\int_{i-1}^{i} \int_{j-\frac{1}{2}}^{j+\frac{1}{2}} \left\{ \frac{\partial \phi}{\partial x} + (a+b\omega) \frac{\partial \varphi}{\partial \omega} \right\} dx d\omega = \int_{j-\frac{1}{2}}^{j+\frac{1}{2}} [\varphi]_{i-1}^{i} \, d\omega +$$

$$\left\{ [a+b\omega]_{j-\frac{1}{2}}^{j+\frac{1}{2}} - b \int_{j-\frac{1}{2}}^{j+\frac{1}{2}} \varphi \, d\omega \right\} dx$$

and $$\int_{i-1}^{i} \int_{j-\frac{1}{2}}^{j+\frac{1}{2}} \frac{\partial}{\partial \omega} \left(c \frac{\partial \varphi}{\partial \omega} \right) d\omega dx = \left\{ \left[c \frac{\partial}{\partial \omega} \right]_{j-\frac{1}{2}}^{j+\frac{1}{2}} \right\} \Delta x$$

where a, b and c are assumed to be constant between stream-wise steps. The above expressions can be evaluated by using the linearized expressions for φ, where

$$\varphi_i(\omega) = \begin{cases} \varphi_{i,j} + (\varphi_{i,j+1} - \varphi_{i,j})(\omega-\omega_j)/(\omega_{j+1} - \omega_j) & \text{if } \omega_j \leq \omega \leq \omega_{j+\frac{1}{2}} \\ \varphi_{i,j} + (\varphi_{i,j-1} - \varphi_{i,j})(\omega-\omega_j)/(\omega_{j-1} - \omega_j) & \text{if } \omega_j \geq \omega \geq \omega_{j-\frac{1}{2}} \end{cases}$$

The final component of the micro-integral equation, that is for the source term, d , requires special consideration and a detailed discussion of this term and its numerical treatment is given in Reference (8). In brief, by defining the term

$$S_{i,j} \equiv \frac{1}{\Delta x} \int_{i}^{i+1} (\psi_E - \psi_I) \int_{j-\frac{1}{2}}^{j+\frac{1}{2}} d\varphi d\omega dx$$

and one can show that

$$S_{i,j} \simeq (1/8)(\psi_E - \psi_I)(\omega_j - \omega_{j-1})(d_{j+1} + d_{j-1} + 6d_j)_{i-1}$$

Having linearized the source term, and assuming a linear variation in φ between adjacent grid points, the above expressions are substituted into the micro-integral equation which, after collecting terms, yields a set of algebraic equations for the generic <u>interior</u> point i,j in the form

$$\phi_{i,j} = A_j \varphi_{i,j+1} + B_j \varphi_{i,j-1} + C_j \qquad (20)$$

$$j = N2-1, N2-2, \ldots N1+1$$

where N2 and N1, respectively, define the grid points at ω=1 and ω=0. The coefficients A_j, B_j and C_j at an interior point (i,j) are defined from the following equations:

$$A_j' = \left[(2)(r_{j+1}-r_j)^{-1} (r\mu_T/\sigma_\phi)_{j+\frac{1}{2}} \right]_{i-1} - \left[(\psi_E - \psi_I)(a + b\omega_{j+\frac{1}{2}}) \right]_{i-1}$$

$$- \left[(1/4)(\psi_E - \psi_I)(1/\Delta x - b)(\omega_{j+1} - \omega_j) \right]_{i-1}$$

$$B_j' = \left[(2)(r_j - r_{j-1})^{-1}(r\psi_T/\sigma_\phi)_{j-\frac{1}{2}}\right]_{i-1} + \left[(\psi_E - \psi_I)(a + b\omega_{j-\frac{1}{2}})\right]_{i-1}$$

$$- \left[(1/4)(\psi_E - \psi_I)(1/\Delta x - b)(\omega_j - \omega_{j-1})\right]_{i-1}$$

$$C_j' = \left\{(1/4)(\psi_E - \psi_I)(\Delta x)^{-1}\left[3\phi_j(\omega_{j+1} - \omega_{j-1}) + \phi_{j+1}(\omega_{j+1} - \omega_j)\right.\right. \qquad (21)$$

$$\left.\left. + \phi_{j-1}(\omega_j - \omega_{j-1})\right]\right\}_{i-1} + 2S_{i,j}$$

$$D_j' = A_j' + B_j' + (\omega_{j+1} - \omega_{j-1})\left[(\psi_E - \psi_I)/\Delta x\right]_{i-1}$$

with

$$S_{ij} = (1/8)(\psi_E - \psi_I)(\omega_j - \omega_{j-1})\{\vec{d}_{j+1} + \vec{d}_{j-1} + 6\,\vec{d}_j\}_{i-1}$$

and $A_j = A_j'/D_j'$, $B_j = B_j'/D_j'$, $C_j = C_j'/D_j$

V.2 Finite Difference Equations: Boundary Points

Values at the end points of the grid network (N2, N1) are prescribed from boundary conditions in the inviscid external stream (ω=1, J=N2, r=r_E) and from either boundary conditions within the unmixed portions of the jet (ω=0, j=1, r_I>0) or symmetry conditions on the axis once the jet becomes fully mixed (ω=0, j=N1+1, r_I=0). For the latter situation Equation (20) is modified by the symmetry statement $\phi_{i,N1} = \phi_{i,N1+2}$ where the grid point (i, N1+1) defines the jet axis; thus, Equation (20) yields

$$\phi_{i,N1+1} = \phi_{i,N1+2}\,(A_j + B_j) + C_j \qquad (22)$$

V.3 Finite Difference Equations: Mass Entrainment

Although the coefficients A_j, B_j and C_j are based upon flow properties at the (i-1) station, matrix inversion of Equation (20) can only proceed once the mass entrainment between stations (i) and (i-1), manifested through the parameters a, b and $(\psi_E-\psi_I)$, is determined. From the discussion of mass entrainment in Section IV, and from Equations (19a) and (19b), it can be readily shown that:

$$(a)_{i-1} = \left[2(\mu_T r)_{N1+3/2} \Big/ (r_{N1+2} - r_{N1+1}) \Big/ (\psi_E - \psi_I) \right]_{i-1}$$

$$(b)_{i-1} = \left[2(\mu_T r)_{N2-3/2} \Big/ (r_{N2-1} - r_{N2-2}) \Big/ (\psi_E - \psi_I) \right]_{i-1} - a_{i-1} \qquad (23)$$

Having calculated the quantities a and b (or equivalently $r_R m_E$ and $r_I m_I$), the change in the stream function $(\psi_E-\psi_I)$ can be found using Equation (19b) where

$$\frac{d}{dx}(\psi_E-\psi_I) = r_I m_I - r_E m_E$$

or, in finite-difference notation,

$$(\psi_E-\psi_I)_i = (\psi_E-\psi_I)_{i-1} \left[1 + (b)_{i-1} \Delta x \right] \qquad (24)$$

The physical r-location of each grid point is determined by inverse quadrature, i.e.,

$$(r-r_I)^2 = 2(\psi_E-\psi_I) \int_o^\omega (\rho u)^{-1} d\omega \qquad (25)$$

which results directly from the physical significance of the stream function, ψ, and the definition for ω.

V.4 Finite Difference Equations: Chemical Production Term

We have tacitly indicated that the introduction of finite-rate kinetics into the investigation of fluid-flow phenomena can lead to a mathematically "stiff" system of equations. For H_2/Air reactions, for example, the physical basis of the "stiffness" results from the importance of the hydroxyl radical in the overall kinetics scheme. Usually, every reaction considered that generates water requires an expenditure of OH radicals. Since the concentration of the OH radical is always small, and since the rate of production of water in H_2/Air systems can be very fast, the coefficients required for the calculation of OH must be very large and intrinsically positive. Thus, the rate of production of OH requires an equation involving differences of very large numbers which mathematically can be shown to be a highly unstable situation when one resorts to standard Runge-Kulta predictor/corrector techniques. As alluded to previously, methods do exist to cope with this problem; the approach used here is discussed by Moretti and Rubel. Following the uncoupling process of Moretti, for each marching step Δx, the specie mass fraction, α_K, which are governed by the differential equation

$$\partial\alpha_K/\partial x + (a+b\omega)\partial\alpha_K/\partial\omega = \partial/\partial\omega(c\partial\alpha_K/\partial\omega) + \dot{w}_K/\rho u \qquad (26)$$

$$K = 1,2, \ldots N$$

is divided into two components $\alpha_K = \alpha_K^{(D)} + \alpha_K^{(C)}$, respectively controlled by the equations

$$\partial\alpha_K^{(D)}/\partial x + (a+b\omega)\partial\alpha_K^{(D)}/\partial\omega = \partial/\partial\omega(c\,\partial\alpha_K/\partial\omega) \qquad (26a)$$

and

$$\partial\alpha_K^{(C)}/\partial x = \dot{w}_K/\rho u \qquad (26b)$$

The numerical solution of Equation (26a) is obtained according to the integration process described above (Equations 20-22). By contrast, Equation (26b) is recast in the subdomain, Δx, with the form

$$\frac{d\alpha_K^{(C)}}{dt} \equiv \frac{1}{u}\frac{d\alpha_K^{(C)}}{dx} = -A_K(T,\alpha_i)\alpha_K + B_K(T,\alpha_j) \qquad (27)$$

$$K = 1,2,3, \ldots N;\ j \neq K$$

upon substitution of the law of mass action (Equation (6)), where the coefficients A_K and B_K are expressed as:

$$A_k = \sum_{m=1}^{R} (\nu_{mk}'' - \nu_{mk}') \{k_{f,m} L_{k,m} \prod_{i=1}^{N} (\rho\alpha_i/W_i)^{\nu_{mi}'} - k_{b,m} (L_{k,m} - 1)^2 \cdot \prod_{i=1}^{N} (\rho\alpha_i/W_i)^{\nu_{mi}''}\} \alpha_k$$

$$B_k = \frac{W_k}{\rho} \sum_{m=1}^{R} (\nu_{mk}'' - \nu_{mk}') \{k_{f,m} (L_{k,m} - 1)^2 \prod_{i=1}^{N} (\rho\alpha_i/W_i)^{\nu_{mi}'} - k_{b,m} L_{k,m} \cdot \prod_{i=1}^{N} (\rho\alpha_i/W_i)^{\nu_{mi}}\}$$

where $L_{k,m} = 1$ if the molecularity of reaction m, for species k, i.e., if $(\nu_{mk}'' - \nu_{mk}')$ is negative or $L_{k,m} = 0$ if the molecularity is positive.

Following the linearization technique of Rubel, the integral of Equation (27), written in the form

$$\alpha_K(\Delta t) = \alpha_K(0)\ \exp\left[- A_K \Delta t \right] + (B_K/A_K)\left[1-\exp\ (-A_K \Delta t) \right] \qquad (29)$$

$$K = 1,2, \ \ldots\ N$$

is determined subject to the requirements that 1) the enthalpy h at the grid-point (i,j) satisfy

$$h_{i,j} = \sum_{K=1}^{N} (\alpha_K/W_K) h_K^{(0)}(T) = (H - 1/2u^2)_{i,j} \qquad (30)$$

where H(i,j) and u(i,j) have already been determined from the implicit integration of Equation (20), and 2) the conservation of chemical elements involved in the N species is preserved (see footnote on page).

The overall change in specie concentration and temperature at the grid point (i,j) is obtained by iteratively solving Equation (29) subject to the constraints imposed by the above two conditions. In particular, the elements of A_K and B_K are initially (in the sense of the iteration loop) determined by considering $T^{(0)} = T_{i,j}^{(D)}$ and $\alpha_K^{(0)} = 1/2\ \ (\alpha_K)_{i-1,j} + \alpha_K{}^{(D)}_{i,j}$ where the superscript connotes the iteration step. Substitution into Equation (29) allows for the predictor calculation of the species α_K, i.e., $\alpha^*_{K_{i,j}}$. The corrector values are obtained by considering

$$(\alpha_K)_{i,k}^{(n+1)} = 1/2\ \ \alpha_K^{(0)} + \alpha_K^{*\,(n)}{}_{i,j}$$

$$T^{(n+1)} = 1/2\ \ T^{(0)} + T^{*\,(n)}$$

where the temperature, T, is determined using Equations (11) and (30). This allows new values of A_K and B_K to be determined and the entire process is repeated until the relative change in temperature from one iteration step to the next becomes less than a prescribed value.

Models of chemical kinetics generally undergo continual updating as applications are extended to newer regimes of chemical behavior. The modifications require the addition of reactions and/or species to the model. A practical aspect of the numerical procedure expounded is the ease with which such changes can be incorporated into the program. This characteristic is a consequence of the uncoupling of the species interactions through Equation (27). Thus, simple modification of coefficients A_K, B_K effect the desired changes in the chemical kinetics model.

V.5 Step Size Controls

For non-reacting turbulent mixing, i.e., $\dot{w}_i=0$, the numerical finite difference formulation is implicit since there is no need for the uncoupling procedure described in the previous section. Accordingly, stability is insured even for large numerical steps; however, reasonably small step sizes are desired for good accuracy. One procedure is to make the step length proportional to the thickness of the mixing layer. A variant to this approach is to make the step length equal to the minimum physical spacing between grid points, i.e.,

$$\Delta x^{(D)} = \left\{ \min \left[r_{j+1} - r_j \right] \right\}_{i-1} \tag{31}$$

For reacting, turbulent flows, the chemical production terms are near-zero and the uncoupling procedure and solution technique renders the system into a hybrid implicit/explicit scheme. The explicit nature for the calculation of

$\alpha_K^{(C)}$ poses an additional step-size constraint on numerical stability and accuracy. Under these conditions, one can show that stability is dictated by the maximum eigenvalue, λ, for the Jacobian matrix $J = \{\gamma_{\ell K}\}$ where $\gamma_{\ell K} = \partial \dot{w}_\ell / \partial \alpha_K$. Difficulties in determining this eigenvalue are reduced if it is assumed that the chemical rates are such that the diagonal element of the Jacobian matrix, γ_{KK} is dominant. Accordingly, the allowable step size can be shown to be

$$\Delta x^{(C)} = u_{jet} \min \left\{ \alpha_K \left(\frac{d\alpha_K}{dt}^{(C)} \right)^{-1} \right\}_{i-1} \tag{32}$$

where $d\alpha_K^{(C)}/dt$ is readily evaluated using Equation (27). In practice, the actual step size taken is determined by combining Equations (31) and (32) according to

$$(\Delta x)_{act} = \left\{ \frac{1}{\Delta x^{(D)}} + \frac{1}{\Delta x^{(C)}} \right\}^{-1} \tag{33}$$

which implies that under diffusion-controlled situations, $\Delta x^{(D)}$ is the predominant factor, while under kinetically-controlled mixing $\Delta x^{(C)}$ determines the marching step.

SECTION VI

KINETIC MECHANISM AND RATE DATA

In starting this section it seems appropriate to discuss first the role of chemical kinetics of the fundamental level in turbulent reacting flows. In complex chemical systems many individual reactions of the type given by Eq. (8) may be involved so that the volumetric role of production, $\dot{w}_i$, given by Eq. (6) and required in the specie conservation equation will contain a large number of terms. For example, for a typical elementary reaction

$$\nu_1 M_1 + \nu_2 M_2 \underset{k_b}{\overset{k_f}{\rightleftharpoons}} \nu_3 M_3 + \nu_4 M_4$$

implementation of Eq. (6) yields

$$f_i = \dot{w}_i / \nu_i W_i = - k_f \rho^{(\nu_1 + \nu_2)} \gamma_1^{\nu_1} \gamma_2^{\nu_2} + k_b \rho^{(\nu_3 + \nu_4)} \gamma_3^{\nu_3} \gamma_4^{\nu_4}$$

where $\gamma = \alpha_i / W_i$. Thus, because it is frequently not possible to take into account all individual reactions and their related rate constants, it is usual in the analysis of complex chemical systems to consider only a few reaction steps, which possibly do not correspond to the proper mechanism of reaction on a molecular scale but which in a gross sense do describe the overall process.

However, there is increased concern in the applicability of overall reaction mechanisms and rates to turbulent flows.[6] Since this global approach does not correspond to chemical behavior at the molecular level, their utilization in turbulent flows with heterogeneities in composition is a subject of continuing investigation in the open literature. To see some of the difficulties arising from the creation term in turbulent flows, consider a simple one step unidirectional reaction

$$M_1 + M_2 \xrightarrow{k} M_3$$

which, in this case

$$\dot{w}_1 = - \rho^2 \, k \, \gamma_1 \gamma_2$$

where the reaction rate, k, is considered to be a function of temperature. Now decomposing each of the elements into a mean ($\bar{}$) and fluctuating term ( )' gives

$$\dot{w}_1 = (\bar{\dot{w}} + \dot{w}') = - (\bar{\rho} + \rho')^2 \, k(\bar{T} + T') \, (\bar{\gamma}_1 + \gamma_1') \, (\bar{\gamma}_2 + \gamma_2')$$

and applying the Eulerian time mean averages yields

$$\bar{\dot{w}}_1 = - \bar{\rho}^2 \, k \, (\bar{T}) \, \bar{\gamma}_1 \bar{\gamma}_2 \, \{1 + [\text{second order and higher correlations}]\}.$$

It has been shown[6,23] that the terms within the square bracket are not necessarily small; and, to model these correlations presently imposes undo restrictions on the assumed kinetics (like the simple one-way reaction posed above). Accordingly, due to this formidable complexity, it will be assumed that for engineering purposes, chemical reactions in turbulent flow occur according to the classical, laminar, kinetic behavior and to depend only upon mean values of species concentration, temperature and density which is tantamount in neglecting the terms in the above square bracket. In this connection, the reaction system and rates, largely extracted from Ref. 24 and listed in Table III are adopted here.

SECTION VII

NUMERICAL/EXPERIMENTAL COMPARISONS - NONREACTIVE TURBULENT MIXING

Substantive progress in modeling turbulent, nonreactive shear flows has been achieved in recent years as indicated in the Proceedings of the 1972 NASA-Langley Conference on Free Turbulent Shear Flows,[7] wherein the state-of-the-art in understanding and describing the basic fluid dynamic aspects of the problem was thoroughly examined. Specifically, for nonreactive flows the Conference Evaluation Committee concluded that differential mean turbulent field methods, like the one just described in this report, represent an approach which promises systematic development toward a practical degree of generality.

Rodi[11] and Launder, et al.[9] have presented the results of many comparisons of numerical predictions based upon the "two-equation model" with experimental data culled from the world's literature. These data are related to steady two-dimensional "parabolic" flows such as plane jets, wakes and mixing layers, wall jets, boundary layers of various kinds, and flows in pipes and annuli. Agreement with experiment varies from good to very good. Several of these comparisons between theory and experiment are shown in Figures 4a through 4f. These figures, largely extracted from Ref. 9, and succinctly summarized in Table IV, favorably compare the numerical predictions in axial velocity decay with various experimental measurements in turbulent axisymmetric jet flows. In particular, Figures 4a and 4b depict comparisons with air/air turbulent nonreactive jets while Figures 4c and 4d display comparative numerical/experimental trends in H_2/air (jet/ambient) turbulent nonreactive jets. Although these latter two figures show reasonable agreement between theory and experiment, Launder, et al. point out that increased disparity between the k-ε2 predictions and measurements arise in flows that have appreciable density gradients.

In cases involving large compressibility effects manifested either by the high speed characteristics of the jet or the marked variation in density between the jet fluid and the surrounding environs, Dash, et al.[25] shows that some improvement in numerical predictions can be achieved if one incorporates a modification to the k-ε2 model. Basically, the modification resides in the fact that the effect of compressibility can be phenomenologically related to a reduction in the turbulence scale and hence in the effective turbulent viscosity μ_τ. Based upon heuristic arguments, this effect depends mainly on the Mach number fluctuation $M_\tau \equiv (k^{\frac{1}{2}}/a)$, where a is the local sound speed (in free jet flows "a" is mainly a function of density) and, in place of Eq. (14) one should use

$$\mu_\tau = C_1 (M_\tau) C_\mu \rho k^2/G \tag{34}$$

where the function $C_1 (M_\tau)$, as presented in Ref. 25, being determined by a systematic comparison of select theoretical calculations and available shear layer experiments. Figures 4e and 4f, taken directly from Ref. 25, show the relative improvement when the aforenoted modification is implemented into the k-ε2 model. Indeed, further clarification in compressibility effects and the generality in the above modification is deemed warranted, albeit, its direct implementation in this analysis is otherwise noted.

SECTION VIII

NUMERICAL PREDICTIONS: REACTIVE TURBULENT MIXING

As a possible prelude to direct application in containment vessel response, several select numerical experiments were performed to check the qualitative behavior of the numerical prediction. Specifically, initial PCRV inventory was presumed composed of 100 moles of CO and H_2 and 5246 moles of He. A jet-to-free-stream temperature ratio of 3.3 was considered with a jet-to-free-stream velocity ratio being either 100 (Test Case No. 1) or 10 (Test Case No. 2); the former approximating the early stages of a nonmechanistically postulated penetration failure; the latter, approximating the final stages of such a failure.

Computer generated plots of the spatial variation of temperature, and mole fraction of CO and H_2 for these two cases are presented in Figures 5, 6, and 7.

A cursory examination of the results portrayed by these figures indicates the following:

(1) For both test cases the initial conditions are such to support a turbulent diffusion flame.

(2) Mixing is more rapid under Test Case 1 conditions (u_j/u_E = 100 @ X=0) then under Test Case 2 conditions (u_j/u_E = 10 @ X=0).

(3) Depletion of CO and H_2 (or production of CO_2 and H_2O) occurs sooner under Test Case 2 conditions where rather sudden changes in the axial temperature gradients occur within the mixing layer about two jet radii downstream as compared to Test Case 1 where large variations in axial temperature are apparent approximately seven jet radii downstream.

(4) The spatial variation of temperature and other variables precludes to some extent the use of analytical similarity distributions which have

been used in the "layering" models found in Ref. 5.

Although these results are highly preliminary, they do tend to indicate that the phenomena of turbulent mixing should be investigated with more recent state-of-the-art models than those which have heretofore been applied to containment atmospheric response studies. In addition, the possibility of diffusive burning of combustibles released either during a depressurization failure or as a direct consequence thereof must be examined with mixing codes directly linked to a chemical kinetics analysis.

In this connection, these general comments and modeling technique have also been substantiated by the recent work of Landoni[26,27] of General Atomic dealing with their containment atmospheric response study program.

SECTION IX

HTGR SAFETY: THE NEED FOR A TURBULENT REACTIVE MIXING ANALYSIS

During the time this report was being written, the author became aware of the containment atmospheric response study program of General Atomic as described by the work of Landoni, et al.[20,27] In the former reference emphasis was placed mainly on the study of turbulent jet structure during a DBDA and its effects on CV pressure and heat loads. The latter work stressed the long term survivability of the secondary containment under conditions of unrestricted core heatup resulting from loss of forced circulation with concomitant production of combustible gases due to concrete decomposition.

The author concurs with the unit problem approach alluded to in these references but wishes to add that, contrary to the conclusions drawn therein, turbulent reactive mixing codes employing a so-called "two-equation" turbulence model can provide the necessary groundwork in modeling turbulent jets. In addition, with some modifications, these models can be extended to include buoyant plumes as well -- restricted, of course, to the parabolicity of the flow. Methods do exist in linking these analytical models with classical phenomenological chemical kinetics codes as is described herein. Of course, these comments must be tempered by the need of additional experimental work of multicomponent gas mixing at conditions closely akin to a DBDA.

REFERENCES

1. Baxter, A. M. and Swanson, L. L. HTGR plant dynamics under accident conditions. Nucl. Eng. & Design 26, 1/1, 103-107 (1974).

2. Peroomian, M. B., Barsell, A. W. and Saeger, J. C. OXIDE-3: A computer code for analysis of HTGR steam or air ingress accidents. GA-A-12493 (GA-LTR-7), General Atomic Company, January 1974.

3. Macnab, D. I. The CONTEMPT-G computer program and its application to HTGR containment. GA-A-12692 (GA-LTR-6), General Atomic Company, February 1974.

4. Palmer, H. B., Sibulkin, M., Strehlow, R. A. and Yang, C. H. An appraisal of possible combustion hazards associated with a high temperature gas cooled reactor. A consultants' report to the BNL HTGR Safety Division, BNL-NUREG-50764, March 1978.

5. Omata, I. An analysis of gas layering and flammability in the containment vessel of an HTGR following depressurization. BNL-NUREG-50622, March 1977.

6. Murthy, S. N. B., Ed. Turbulent Mixing in Nonreactive and Reactive Flows, Plenum Press, New York, 1975.

7. Free Turbulent Shear Flows, Vol. 1, Conf. Proc., NASA SP-321, 1973.

8. Launder, B. E. and Spalding, D. B. Lectures in Mathematical Models of Turbulence, Academic Press, London and New York, 1972.

9. Launder, B. E., Morse, A., Rodi, W. and Spalding, D. B. "Prediction of free shear flows. A comparison of the performance of six turbulence models" in Free Turbulent Shear Flows, Vol. 1, Conf. Proc., NASA SP-321, pp. 361-426, 1973.

10. Bradshaw, P., Ed. Turbulence, Topics in Applied Physics, Vol. 12, Springer-Verlag, 1976.

11. Rodi, W. The prediction of free turbulent boundary layers by use of a two-equation model of turbulence. Ph.D. thesis, University of London, 1972.

12. Patankar, S. V. and Spalding, D. B. Heat and Mass Transfer in Boundary Layers, 2nd Ed., Intertext Books, London, 1970

13. Harsha, P. T. Free turbulent mixing: A critical evaluation of theory and experiment. AEDC Rept. TR-71-36, February 1971.

14. Patankar, S. V. and Spalding, D. B. A finite-difference procedure for solving the equations of the two-dimensional boundary layer. Intern. J. Heat Mass Transfer 10, 1389-1411 (1967).

15. MacCormack, R. W. The effect of viscosity in hypervelocity impact cratering. AIAA Paper 69-354, 1969.

16. Curtiss, C. F. and Hirschfelder, J. O. Integration of stiff equations, Proc. Natl. Acad. Sci. 38, 235-243 (1952).

17. Emanual, G. Problems underlying the numerical integration of chemical and vibrational rate equations in near equilibrium flow. AEDC TDR-63-82, Arnold Engineering Development Center, Tullahoma, Tenn., 1963.

18. Thomas, P. D. and Wilson, K. H. Efficient computation of "stiff" chemically reacting flow in turbulent free jets. AIAA 2nd Computational Fluid Dynamics Conference, June 1975.

19. Boccio, J., Weilersteain, G. and Dash, S. A computational system for the prediction of low altitude rocket plume flow fields. Vol. III - Mixing/ Afterburning Model. GASL TR-239, General Applied Science Laboratories, Westbury, New York, 1976.

20. Ferri, A., Moretti, G. and Slutsky, S. Mixing processes in supersonic combustion. J. Soc. Ind. Appl. Math. 13, 229-258 (1965).

21. Rubel, A. Swirling jet turbulent mixing and combustion calculations. ATL TR 180, Advanced Technology Laboratories, October 1972.

22. Magnus, D. and Schecter, H. Analysis and application of the PADE approximation for the integration of chemical kinetic equations. GASL TR-642, General Applied Science Laboratories, March 1967.

23. Libby, P. A. and Williams, F. A. "Turbulent flows involving chemical reactions" in Annual Review of Fluid Mechanics, Vol. 8, Ann. Reviews, Inc., 1976.

24. Baulch, D. L., Drysdale, D. D., Horne, D. G. and Lloyd, A. C. Evaluated Kinetic Data for High Temperature Reactions, Butterworths, London, 1972.

25. Dash, S., Weilerstein, G. and Vaglio-Laurin, R. Compressibility effects in free turbulent shear flows. AFOSR-TR-1436.

26. Landoni, J. A., DelBene, J. V. and Deremer, R. K. Containment Atmospheric Response (CAR) Program Interim Summary Report, ERDA Report GA-A-14262, General Atomic Company, May 1977.

27. Landoni, J. A. Containment Atmospheric Response (CAR) Program Status Report, ERDA Report GA-A-14699, General Atomic Company, February 1978.

TABLE I

The Energy Dissipation Turbulence Model (kε2)

$$-\rho\overline{uv} = \mu_T \frac{\partial u}{\partial y}$$

$$\mu_t = C_\mu \rho k^2/\varepsilon$$

$k \equiv$ turbulence kinetic energy $= 1/2(\overline{u_i u_i})$

$\varepsilon \equiv$ turbulence dissipation $= \mu_t \sum \overline{(\partial u_i/\partial x_j)^2}$

$\mu_t \equiv$ effective turbulent viscosity

C_μ	$C_{\varepsilon 2}$	$C_{\varepsilon 1}$	σ_K	σ_ε
*	**	1.40	1.0	1.3

* $C_\mu = 0.09\, g(\overline{P/\varepsilon}) - 0.0534$

$$(P/\varepsilon) = \int_{r_I}^{r_E} \rho\overline{uv}\,(P/\varepsilon) r dr \Big/ \int_{r_I}^{r_E} \rho\overline{uv}\, r dr$$

$P \equiv$ turbulence energy production $= \mu_t (\partial u/\partial y)^2$

$$g(\overline{P/\varepsilon}) \simeq 1/(\overline{P/\varepsilon})$$

** $C_{\varepsilon 2} = 1.94 - 0.134 f$

$$f = \left| \frac{(0.5)(\Delta r)}{\Delta u} \left(\frac{du_{CL}}{dx} - \left| \frac{du_{CL}}{dx} \right| \right) \right|^{0.2}$$

TABLE II

Source Terms in Transform Equations

ϕ	σ_ϕ	d_ϕ
u	1	$(1/\rho u)\ \{gr_j/u_j^2(\rho_e-\rho) - (\phi_j/\rho_j u_j^2)\ dp/dx\}$
H	Pr_t	$(u_j^2/H_j)\ \partial/\partial\omega\ \{[\rho u r^2 \mu_t/\Delta\psi^2](1 - 1/Pr)\ \partial/\partial\omega\ (u^2/2)\}$
k	σ_k	$(1/\rho u)\ \{[\rho^2 u^2 r^2\ \mu_t/\Delta\psi^2]\ (\partial u/\partial\omega)^2 - \rho\varepsilon\}$
ε	σ_ε	$(1/\rho u)\ \{[\rho^2 u^2 r^2\ C_{\varepsilon_1}\ \mu_t/\Delta\psi^2]\ (\varepsilon/k)\ (\partial u/\partial\omega)^2 - C_{\varepsilon_2}\ \rho\varepsilon^2/k\}$
α_i	Sc_t	$(1/\rho u)\ \{\dot{w}_i\}$ $\quad i = 1,2, \ldots N-L$
$\tilde{\alpha}_j$	Sc_t	0 (see note below)

Note: The L differential equations for $\tilde{\alpha}_j$ can be replaced by L algebraic equations by invoking the conservation of elements, i.e.,

$$\tilde{\alpha}_\ell = \Sigma\ \mu_{k,\ell}\ \alpha_k\ W_\ell/W_k \qquad \ell = 1,2, \ldots L$$

where $\mu_{k,\ell}$ defines the number of atoms of element, ℓ, in species, k. The differential equations for $\tilde{\alpha}_\ell$ have relevance in chemical equilibrium flows where the $\dot{w}_i$ in the specie conservation equations are mathematically undefined.

TABLE III

Chemical System (He/H/C/O/N)

Reaction Number/Chemical Reaction	Forward Rates $k_f = AT^N \exp(-E/RT)$		
	A	N	E/R
1. $CO + O + M \rightleftarrows CO_2 + M$	6.1E-33	0	1872
2. $CO + O \rightarrow CO_2$	1.4E-18	0	1308
3. $CO + OH \rightleftarrows CO_2 + H$	2.5E-17	1.3	-388
4. $H_2 + OH \rightleftarrows H + H_2O$	3.6E-11	0	2607
5. $H + O_2 \rightleftarrows OH + O$	3.7E-10	0	8505
6. $OH + OH \rightleftarrows H_2O + O$	1.0E-11	0	554
7. $O + H_2 \rightleftarrows OH + H$	3.0E-14	1	4509
8. $H + H + M \rightleftarrows H_2 + M$	1.8E-30	-1	0
9. $O + O + M \rightleftarrows O_2 + M$	3.8E-30	-1	171
10. $O + H + M \rightleftarrows OH + M$	2.0E-32	0	0
11. $OH + H + M \rightleftarrows H_2O + M$	6.1E-26	-2	0

(1) Species order: H_2, CO, CO_2, H_2O, H, N_2, O_2, O, OH, He

(2) [A] = $cm^{3n}/(particles)^n/sec$
n = 1 for second-order reactions
= 2 for third-order reactions

(3) M = third body or collision partner

TABLE IV

Initial Conditions for Nonreactive Test Cases

Test Case	Jet Gas	D_j, in.	ρ_j, lb/ft^3	U_j, ft/sec	U_e, ft/sec	U_j/U_e	$(\rho U)_j/(\rho U)_e$	M_j	M_e
6	Air	2.44	0.0818	211.2	0	∞	∞	0.65	0
7	Air	1.01	1.1501	1769.0	0	∞	∞	2.22	0
9	Air[a]	0.25	0.0695	120.0	30.0	4.0	3.7	0.10	0.03
10	H_2	0.50	0.0055	3300.0	517.0	6.3	0.56	0.79	0.421
12	H_2	0.46	0.00601	3524.0	1293.0	2.72	0.163	0.89	1.32
13	Air	0.19[b]	0.0695	120.0	36.4	3.29	3.29	0.10	0.03

a. 10 percent helium tracer by volume

b. 20 jet, 0.19 inch nozzle width

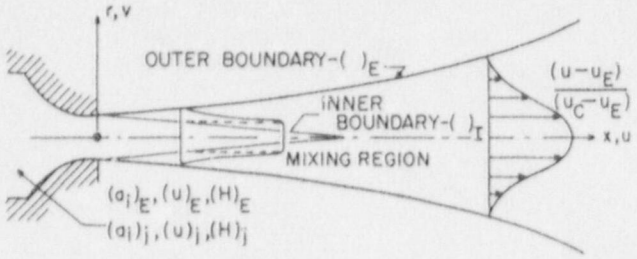

Figure 1. Schematic of mixing flow region.

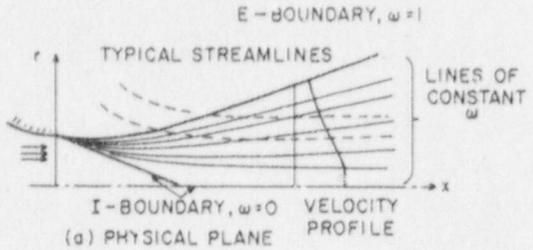

Figure 2. Sketch of axisymmetric jet in physical and mapped coordinate system.

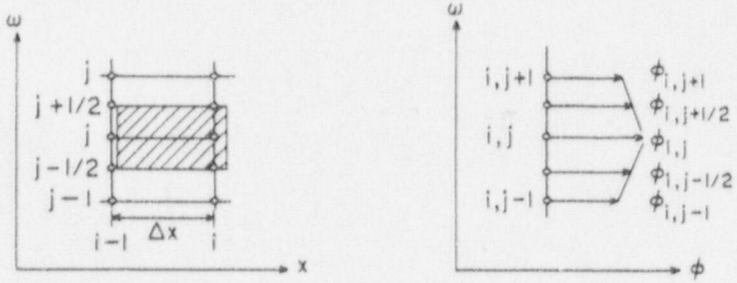

ϕ varies linearly between adjacent cross-stream steps, i.e., $\omega = \omega_{i,j+\frac{1}{2}}$: $\phi = \frac{1}{2}(\phi_{i,j} + \phi_{i,j+1})$.

ϕ varies in a stepwise manner between adjacent streamwise steps, i.e., $x_{i-1} < x \leq x_i$: $\phi = \phi_{i,j}$.

Figure 3. Details of control volume for an interior point.

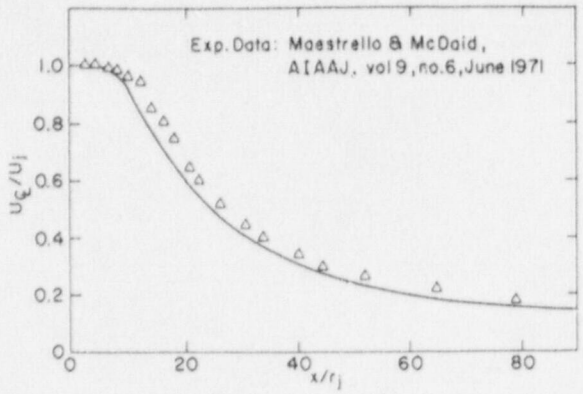

Figure 4a. Comparison, theory/experiment, axial velocity decay - NASA Test Core 6.

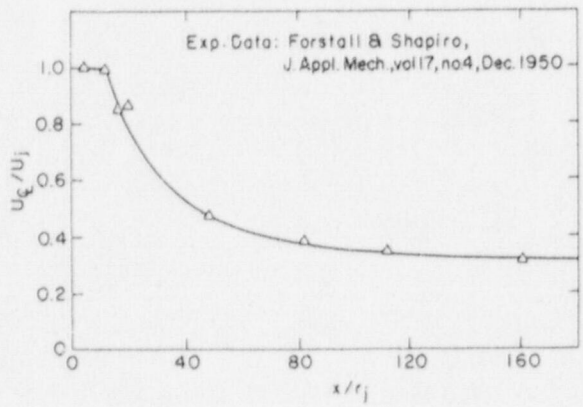

Figure 4b. Comparison, theory/experiment, axial velocity decay - NASA Test Core 9.

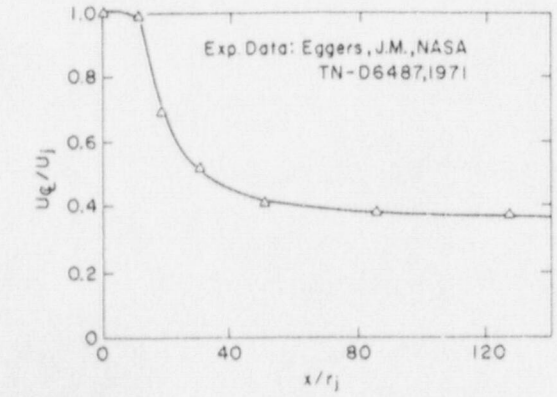

Figure 4c. Comparison, theory/experiment, axial velocity decay - NASA Test Core 12.

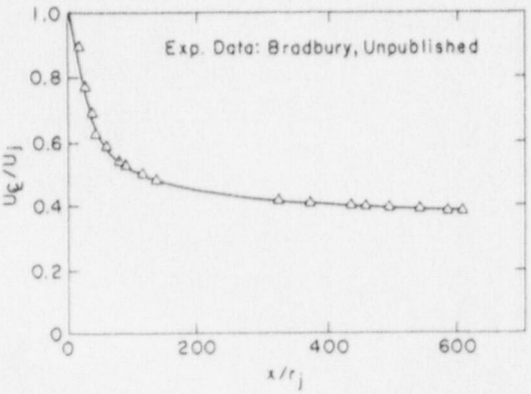

Figure 4d. Comparison, theory/experiment, axial velocity decay - NASA Test Core 13.

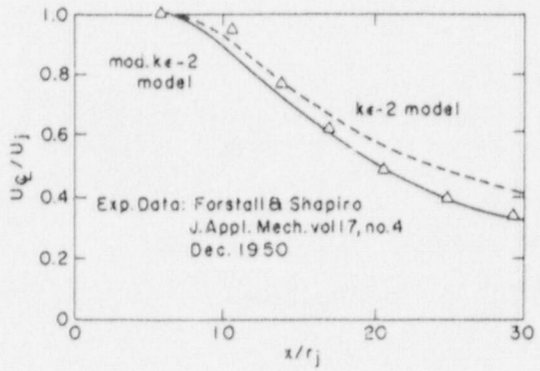

Figure 4e. Comparison, theory/experiment, axial velocity decay - NASA Test Core 10.

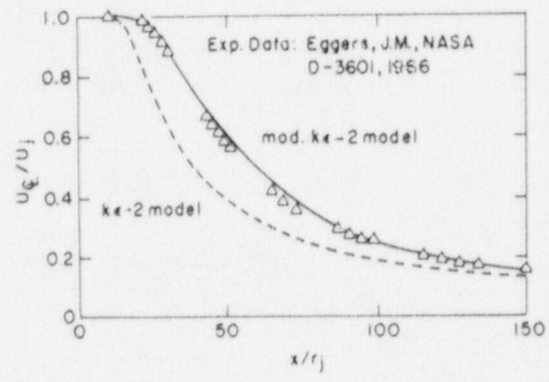

Figure 4f. Comparison, theory/experiment, axial velocity decay - NASA Test Core 7.

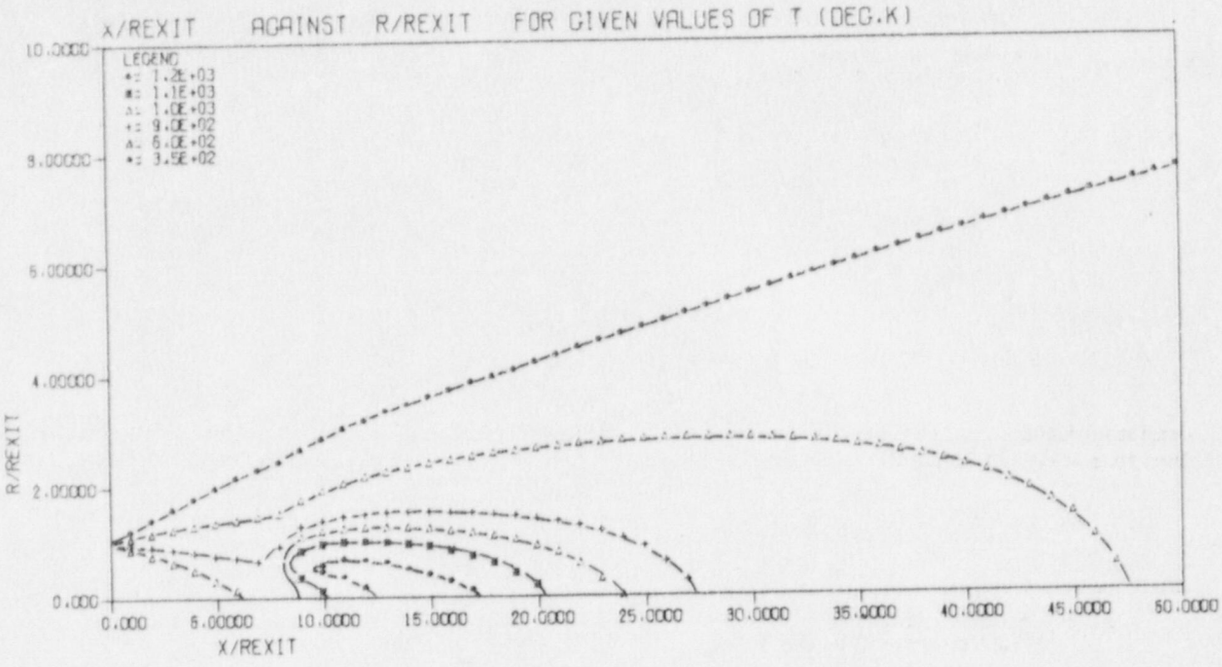

Figure 5a. Computer-generated plot, Test Case 1, temperature.

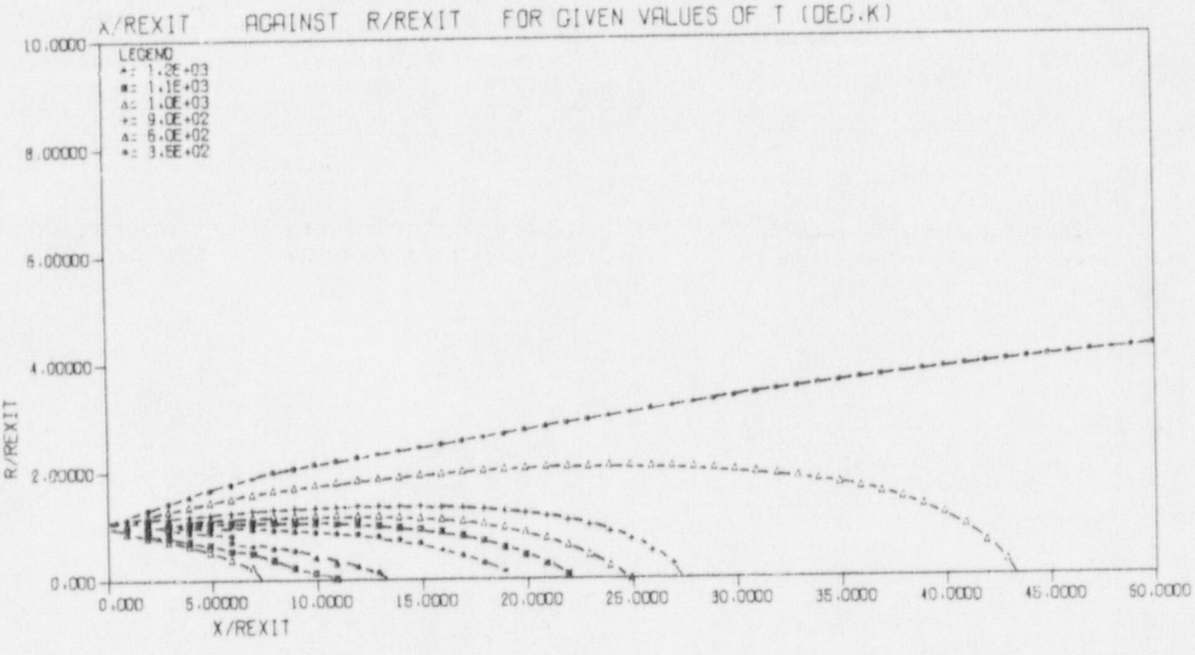

Figure 5b. Computer-generated plot, Test Case 2, temperature.

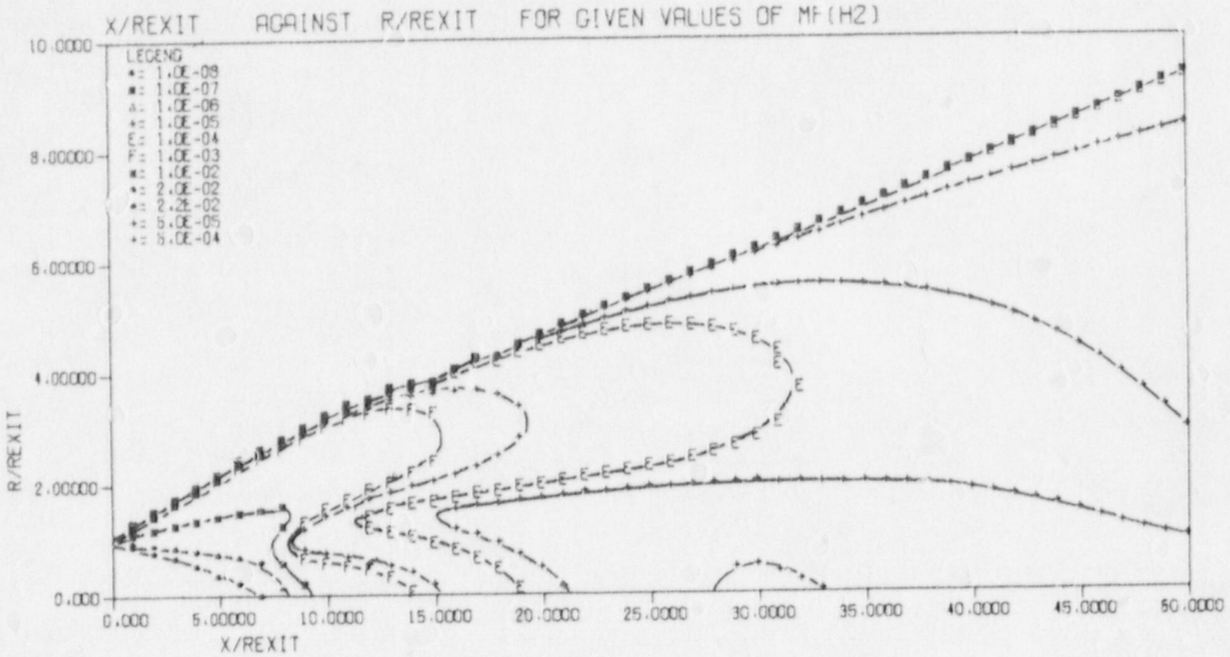

Figure 6a. Computer-generated plot, Test Case 1, H_2 mass fraction.

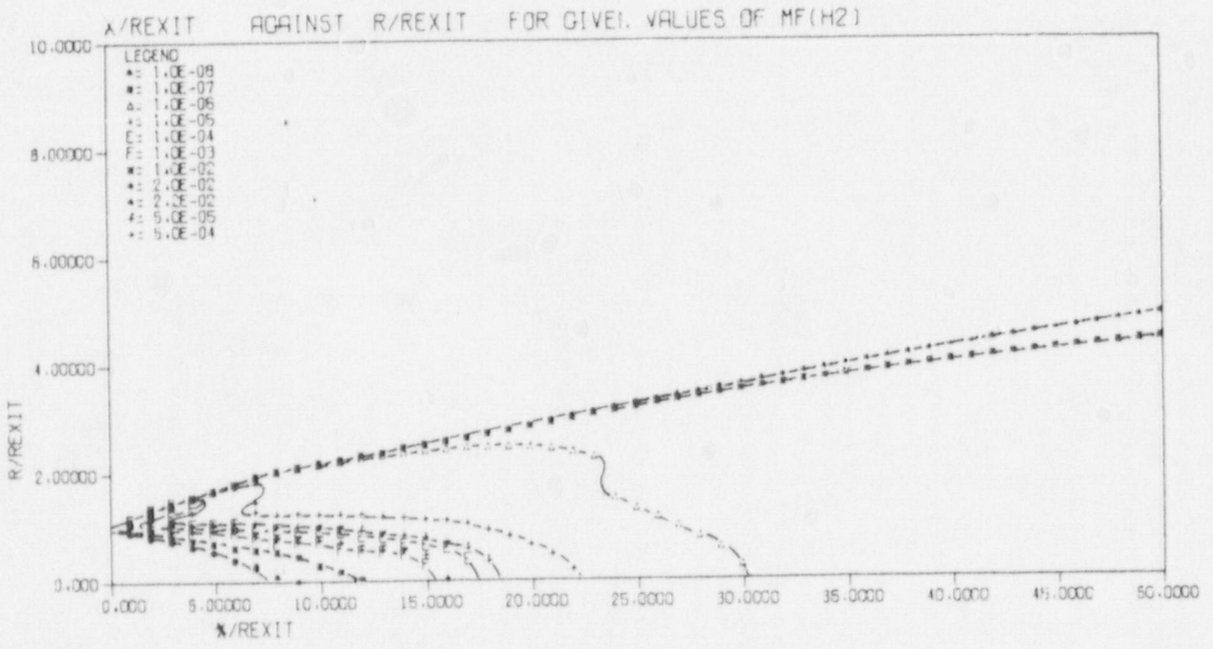

Figure 6b. Computer-generated plot, Test Case 2, H_2 mass fraction.

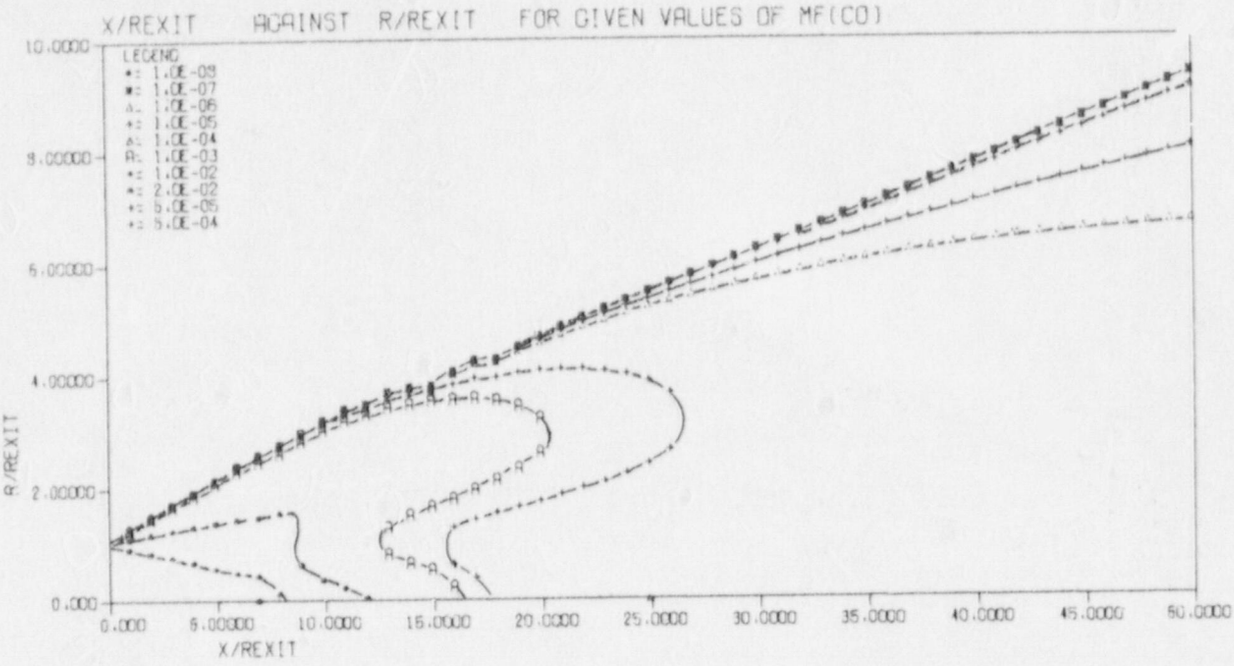

Figure 7a. Computer-generated plot, Test Case 1, CO mass fraction.

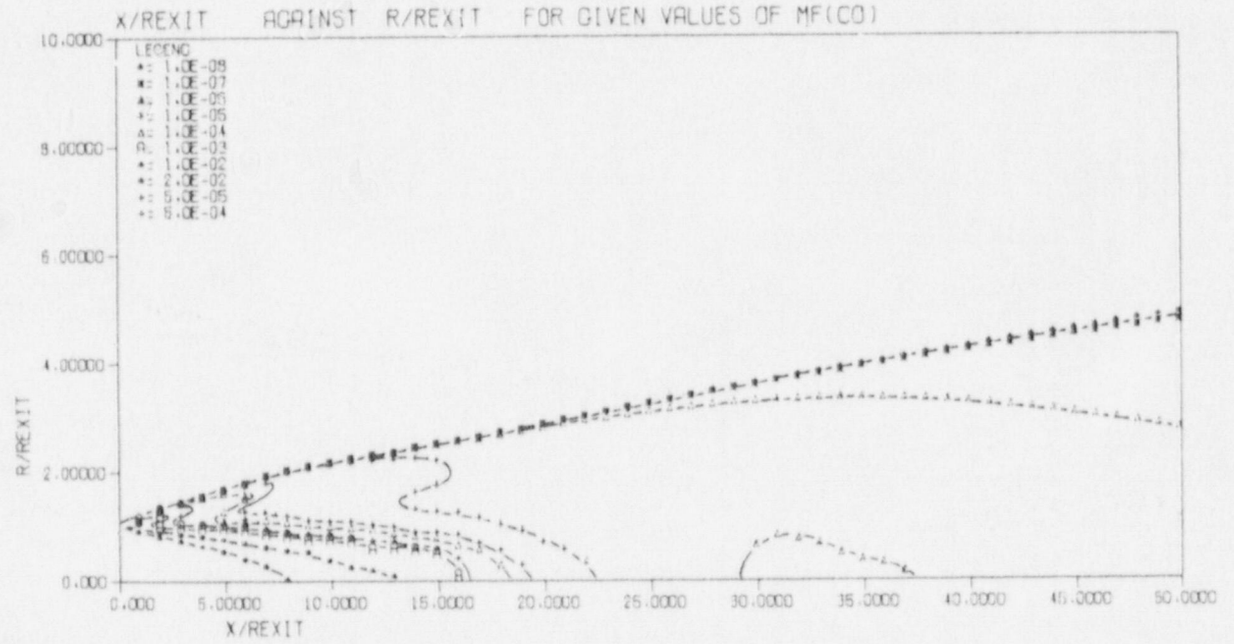

Figure 7b. Computer-generated plot, Test Case 2, CO mass fraction.